Hindawi
Modelling and Simulation in Engineering
Volume 2022, Article ID 4179612, 16 pages
https://doi.org/10.1155/2022/4179612

Research Article

Performance Evaluation of a Photovoltaic-Thermal Collector Coupled Stepped Solar Still for Indian Climatic Conditions

Ayush Narang,[1] Siddhartha Roy,[1] Tarun Kataray,[1] Vishal Bonde,[1] S. Rajesh,[1] C. Chiranjeevi,[1] Utkarsh Chadha,[1,2] and Bulcha Bekele Hirpha[3]

[1]*School of Mechanical Engineering, Vellore Institute of Technology, Vellore, India*
[2]*Department of Materials Science and Engineering, Faculty of Applied Sciences and Engineering, School of Graduate Studies, University of Toronto, Toronto, ON, Canada M5S 2Z9*
[3]*College of Natural and Computational Science, Department of Physics, Dambi Dollo University, Dembi Dolo, Ethiopia*

Correspondence should be addressed to C. Chiranjeevi; chiranjeevi.nit@gmail.com and Bulcha Bekele Hirpha; bulchabekele1@gmail.com

Received 8 September 2022; Revised 29 September 2022; Accepted 5 October 2022; Published 18 November 2022

Academic Editor: Paolo Iodice

Freshwater scarcity is increasing across many parts of the globe; to meet this demand, seawater desalination is the best choice, and the electrical energy consumption is escalating due to urbanization and industrialization. Sustainable production of electricity and freshwater can be met by an integrating photovoltaic-thermal (PVT) module with stepped solar still (SSS). The present study focuses on the theoretical modeling of the PVT-SSS desalination system for evaluating thermal efficiency, energy efficiency, freshwater productivity, and electrical power generation. The solar still productivity will be influenced by the depth of water, insulation thickness, glass cover material, thickness and inclination, and operational factors like preheating the input water supply and water salinity. A comparative analysis has been made of summer, winter, and rainy climatic conditions of Vellore town (12.9165° N, 79.1325° E), Tamil Nadu. In the present work, a thermodynamic model based on mass and energy balance is developed for the PVT-SSS system, and it is solved by a numerical method. A Runge-Kutta technique of 4th order is employed using a Python program for solving the thermodynamic simulation model. The results from the model depict that for summer, winter, and rainy climatic seasons, the freshwater productivity of PV/T-SSS was determined to be 12.18 kg/m^{2}day, 6.67 kg/m^{2}day, and 2.77 kg/m^{2}day. Also, it is found that electrical efficiency for summer, winter, and rainy seasons is 8.91%, 9.135%, and 9.53%, respectively. A maximum and minimum freshwater production of 1668 kg/m^2 and 1218 kg/m^2 are observed for a depth of 2 cm and 5 cm, respectively.

1. Introduction

Freshwater scarcity is one of the key issues that most developing countries are encountering. Freshwater is utilized for various activities, including drinking and cleaning. Water is also utilized to generate electricity and for agriculture irrigation. Rivers and lakes are the primary sources of this freshwater which account for around 2% of the world's total water supply. Around the world, roughly 400 million cubic meters of freshwater are frozen in glaciers, ice caps, and snow cover, leaving us with just about 0.6 percent freshwater available for consumption, which is insufficient to meet the demands of the whole population. Freshwater is not always easily available for human consumption: extracting significant amounts from rivers (particularly in dry locations) may be difficult, and groundwater extraction can harm marine life by altering salt levels in ocean basins. Experts also fear that future climate change could result in less rainfall and excessive groundwater use, perhaps leading to an unprecedented global depletion of freshwater reserves. By 2025, the world's population is expected to cross 8 billion people, resulting in a 56 percent increase in demand for freshwater resources. Due to such low availability of freshwater sources, there are 18 nations where more than half of the population lives in places where water shortage is a daily concern [1]. Because of urbanization and rising water demands brought on by population growth, the level of groundwater is now declining. Given that the Indian coast is relatively long both east and west, desalination plants have a lot of potential and space for expansion [2]. Around 750 million people worldwide lack access to clean drinking water [3]. 82% of those without access to drinking water reside in rural regions, while 18% do so in urban areas. Millions of women and children in rural regions of developing 45 countries spend 140 million hours every day fetching water from distant, often dirty sources, including people who use groundwater and other natural water sources as their drinking water [3, 4]. The integrated energy system is a quick fix for the nation's power and energy shortage and provides society with several positive outcomes. Additionally, it reduces reliance on electricity for daily necessities [5].

Also apart from the freshwater, the electricity demand is steadily increasing in the state political scenario (STEPS). There will be a slight shift from coal, and renewable energy will increase from less than 30% of production in 2020 to more than 40% in 2030. Fulfilling all announced promises would lead to a further 40% increase in demand for electricity by 2050: accelerate the shift away from coal in the production mix and increase the share of renewable energy to about 45% by 2030 [6].

One of the most significant worldwide issues of the twenty-first century is the conservation of the environment and the climate. Clean energy and energy efficiency are potential solutions to this problem. Heat pumps are a venerable technology that are often used for domestic and industrial heat purpose. In addition, heat pumps are an energy-efficient way for enterprises to satisfy their hot water needs [7].

As a novel and promising approach to high-efficiency solar energy usage, the photothermal effect is used to integrate the cogeneration of freshwater and electricity. Flexible MnO/C nanoparticle-based sun evaporators are built in order to achieve both thermoelectricity and interfacial solar evaporation at the same time. The dual-purpose solar evaporator uses low-grade heat from water evaporation to carry out its functions under three sun irradiations. The thermoelectric conversion produced a maximum output voltage of 330 mV. This work shows the promise of adaptable and robust solar evaporators for the cogeneration of freshwater and power not only assisting in the upcycling of waste plastics and the pursuit of carbon neutrality but also creating chances for massive solar energy supplies that are sustainable [8].

A viable method for addressing both the energy and water challenges at once is to effectively harvest solar energy for the creation of steam and electricity. However, the construction of efficient and easy scale-up photothermal materials for steam and electricity cogeneration remains challenging. More importantly, during solar evaporation, the hybrid device produces an open-circuit voltage of 0.3 V and a power output of $1.6\,\mathrm{W\,m^{-2}}$ under 3 sun irradiation. Therefore, the integrated device with synergistic solar thermal utilisation opens up a green way toward simultaneous solar vapor and electric power generation in remote and resource-constrained areas [9].

All living things need freshwater, although it only makes up 2% to 3% of the world's total water supply. Scientists and technicians are paying more attention to revolutionary low-cost desalination methods as a result of the worrying global freshwater reserve depletion. More freshwater is needed for daily requirements due to population growth, increased industrialization, and urbanization; this need can be satisfied through seawater desalination [10].

Desalination is a technique that can ensure water security by reducing demands on aquifers and surface waters, thereby reducing both economic and social concerns. Direct solar desalination might be a viable option for domestic water production, particularly in deserts and isolated places. Various technologies include multistage flash (MSF), multieffect distillation (MED), vapor compression (VC), humidification dehumidification (HD), reverse osmosis (RO), ion exchange (IE), electrodialysis (ED), and solvent extraction (SE) for seawater desalination. However, these technologies are costly, especially when a large amount of freshwater production is not desirable. And using conventional energy sources (fossil fuels) to drive these systems has harmful environmental impacts. Renewable energy sources like the sun, wind, geothermal, biomass, and ocean have been able to partially meet the world's energy needs. One of the most significant sources of renewable energy that can take the place of fossil fuel energy, which contributes to global warming, is solar energy. Solar energy is also cheap and plentiful. Thus, especially in rural or isolated areas, solar desalination is the most suitable renewable technology with no contamination [11].

Studies have proven that solar distillation stills may use solar energy to purify contaminated lakes [12, 13], sea water [14], and groundwater [15] to provide drinkable water for distant, coastal, and rural locations.

The more effective solar-powered technology for extracting potable water out of saline water is solar still. In rural areas, without access to power, this configuration can be combined efficiently. One of the criteria for improving the solar still's output or the distilled water was found to be raising the temperature of the water that is already present in the solar still [16]. But solar stills are having poor efficiency for converting saline water into potable water, so to increase the evaporative rate and productivity of freshwater, we can choose stepped solar stills. A popular and affordable solar still system called tiered solar still provides more freshwater than a basin-type solar still. Due to the thinner water layer and forced flow concept, the evaporation rate in stepping stills is noticeably greater [17]. Several studies have been conducted on the performance analysis of step solar stills; PV- and PVT-based desalination has been performed in recent years. Since they convert solar radiation into electrical energy, solar photovoltaic systems are one the sustainable energy sources. They currently have a lot of promise to fulfil the expanding energy demands of cities. The most extensively advertised systems are solar PV systems [18]. The performance of PV modules is further impacted because a substantial amount of the solar energy that reaches them is converted into thermal energy at high temperatures [19]. The overall amount of energy generated by PV modules decreases as a result of the PV modules' temperature rising, which also causes a large fall in voltage and a modest rise in the current [20]. To enhance the performance of PV modules, passive and active cooling approaches are utilized [21]. Active cooling of PV modules needs a power source to increase the rate of heat transfer between the PV modules and the cooling medium. During the active cooling methods, a pump is used for liquid-based cooling, and a fan is used for air-based cooling [22].

In order to analyse the thermodynamic performance of a novel screw expander-based solar thermal energy plant, this article offers key ideas. The solar electricity generation system proposed in this paper is based on the steam Rankine cycle: water is used as working fluid and storage parabolic trough collectors are used as a thermal source, and screw expanders are used as power machines. Since screw expanders can operate at off-design working conditions in several situations when installed in direct steam generation solar plants, studying expander performance under fluctuating working situations is a crucial issue. The major objective of the current work is to develop a thermodynamic model to investigate the energy advantages of the suggested power system under off-design operating conditions and fluctuating solar radiation [23].

This study suggests a novel solar thermal plant that may provide mechanical power using an improved arrangement of heliostats with solar receivers of the Scheffler type linked with screw-type steam expanders. Scheffler receivers appear to perform better than parabolic trough collectors due to the high compactness of the focal receiver which minimises convective and radiative heat losses even at high vaporization temperatures. At the same time, steam screw expanders are volumetric machines that can be used to produce mechanical power with satisfactory efficiency also by admitting two-phase mixtures and with further advantages compared to steam turbines: low working fluid velocities, low operating pressures, and avoidance of overheating. In this study, a novel direct steam solar power plant based on an SRC is proposed. Water is used as the working fluid and heat transfer medium, while Scheffler solar receivers are used as the thermal source and work-producing machinery, respectively [24].

Saline water absorbs heat, due to which the temperature of the solar PV is reduced. Also, the efficiency of the active hybrid desalination system's PV cell is increased due to the decreased temperature of PV cell walls. As a result, the monocrystalline active hybrid solar desalination system has a total thermal and electrical efficiency of 25% higher than the standard passive system [25].

Sensitivity analysis was carried on a hybrid photovoltaic-thermal water heating system with natural circulation of water by Ji et al. The study reveal that solar photovoltaic system converts solar radiation into electrical energy with a peak efficiency of 9–15%, depending on the solar cell type. More than 80% of solar light falling on photovoltaic (PV) cells is reflected or converted to heat energy rather than converted to electricity. As a result, hybrid photovoltaic and thermal (PV/T) collectors have been developed to generate both energy and heat [26]. Kumar and Tiwari carried out life cycle analysis of a single slope hybrid PVT active solar still and observed that the daily yield of freshwater from the hybrid still is 3 and 5 times higher than that of the passive solar still [27].

From the extensive literature review, it is concluded that numerous works were carried out on conventional solar stills, PVT systems, PVT solar still systems, and a few works on PVT stepped solar stills. Studies related to PVT-SSS systems for different locations are not reported; hence, the performance of assessment is the main topic of the current research is PVT-SSS systems for different seasons for Vellore town, India, climatic conditions. A thermodynamic model is developed to estimate freshwater productivity, electricity generation, and the efficiency of the system. The model is validated with the experimental data reported in the literature, and the results are compared for the three climatic conditions.

2. Methodology

In the system, Figure 1 shows the pumping saline water into the PV/T collector from the water tank, which acts as a preheater that increases the evaporation rate of saline water as the temperature rises. PV cells in the collector supply electricity to pump the saline water. To provide extra additional pumping power, a separate pump is used. When sunlight enters the still through the glass cover, it is enclosed by the absorber plate and it absorbs the heat. Furthermore, the heat from the absorber plate is received by the water, increasing the temperature even more. Evaporative vapor forms when salty water that runs down the stairs condenses. After the vapor condenses on the inner side of the glass cover, desalinated freshwater is created. Figures 2 and 3 shows the energy distribution and water and energy flow in SSS and PVT systems, respectively.

2.1. Technical Specifications. Various instruments were already used to measure performance and productivity depending on the parameters [11]. The temperatures of different components of still such as water, glass surface, and basin have been measured by calculating from the energy equations such that the weather conditions, wind velocities, and the ambient outside temperatures recorded were used as constant parameters. The results are in agreement with that of existing literature after validation and evaluation of comparative analysis.

2.2. Theoretical Considerations. The basin plate's energy balance [28] is

$$I(t)A_b\alpha_b = m_b c_{pb}\left(\frac{dT_b}{dt}\right) + Q_{c,b-w} + Q_{\text{loss}}. \tag{1}$$

The saline water's energy balance [28] is

$$I(t)A_w\alpha_w + Q_{c,b-w} = m_w c_{pw}\left(\frac{dT_w}{dt}\right) + Q_{c,w-g} + Q_{r,w-g} + Q_{e,w-g}. \tag{2}$$

The glass cover's energy balance [28] is

$$I(t)A_g\alpha_g + Q_{c,w-g} + Q_{r,w-g} + Q_{e,w-g} = m_g c_{pg}\left(\frac{dT_g}{dt}\right) + Q_{r,g-\text{sky}} + Q_{c,g-\text{sky}}. \tag{3}$$

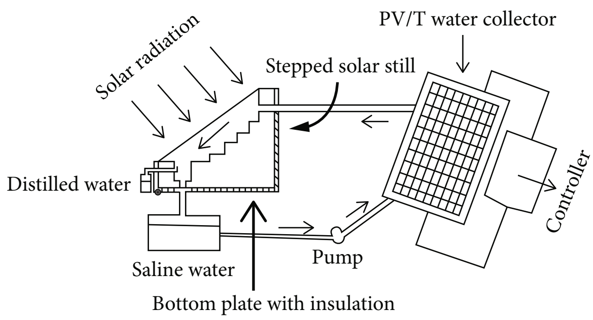

Figure 1: A hybrid PVT-SSS system is depicted.

Equation (4) may be used to calculate the theoretical hourly yield (m_{ew}) [28].

$$m_{ew} = \frac{A_w Q_{e,w-g} 3600}{h_{fg}}. \tag{4}$$

Equation (5) may be used to calculate solar still's efficiency [28].

$$\eta_o = \frac{m_{ew} \times hfg}{A \times I(t)}. \tag{5}$$

Equation (6) is the general form of energy balance relation [11].

$$\sum \dot{E}n_{in} - \sum \dot{E}n_{out} = \left(\frac{dEn}{dt}\right)_{cv}. \tag{6}$$

Equation (7) denotes the energy balance equation for the absorber plate [11].

$$\tau_g \tau_w \alpha_p G_s A_p - h_{p-w} A_p (T_p - T_w) - h_{p-a} A_p (T_p - T_a) = m_p C_p \frac{dT_p}{dt}. \tag{7}$$

Evaporative rate energy and productivity is calculated in [28, 29]

$$En_{ev} = h_{ev,w-g} A_w (T_w - T_g), \tag{8}$$

$$m_{ev} = \frac{En_{ev} \times 3600}{hfg}. \tag{9}$$

The electrical power output of the PVT water collector is in [11]

$$En_{el} = \alpha_c \tau_g A_c G_s \eta_{el,ref} [1 - 0.0045 (T_c - T_{a,ref})] - \frac{\dot{m}_w \Delta P}{\rho_w \eta_{pump}}. \tag{10}$$

The electrical performance of PV/T-SSS is [11]

$$\eta_{el} = \frac{En_{el}}{\tau_g \alpha_c A_c G_s}. \tag{11}$$

3. Validation

Unknown variables were solved using the Runge-Kutta method and validating the current literature's thermal model about experimental data [11]. The design parameters are mentioned in Tables 1–3. The equation gives an average relative error that may be used to compare simulation results to experimental data [29].

$$\mathrm{Er} = \frac{1}{n} \sum_{i=1}^{n} \left| \frac{X_{sim,i} - X_{exp,i}}{X_{exp,i}} \right| \times 100, \tag{12}$$

where n is the number of experimental trails and X is simulated and experimental data.

Table 4 shows the comparison between the experimental results with the existing model. The analytical and experimental data show the same pattern as solar radiation intensity changes. T_c, t_w, and m_{ev} have average relative errors of 0.62%, 1.99%, and 6.77%, respectively. The analytical outcomes of our mathematical model and Naroei et al.'s [11] experiment findings are in good agreement. The theoretical solution techniques and mathematical model are hence reliable. The difference between the experimental results and the mathematical model is shown in Figures 4–6. These figures further validate the current mathematical model [30–32].

The daily production of freshwater is indicated in Figure 4. Theoretical and experimental parameters of the stepped solar still with PV/T are compared in this image. The graph shows that there is an average error of 6.77 between the parameter's experimental and theoretical values.

The average error between the theoretical and experimental parameters shown in Figure 5 plot of PV/T collector temperature vs. time is 0.62%.

The actual and simulated values of the temperature of salted water with time are shown in Figure 6. The average difference between the parameter's experimental and theoretical values is 1.99%.

4. Results and Discussions

4.1. Design Approach. PVT water collection stepped solar still (SSS), pump, and other equipment are part of the experimental setup. From 8 AM to 5 PM, the results are being validated. Half-hour intervals were used to record test data in Vellore. The thermal model is created, and the data is evaluated using information from the literature.

4.2. Mathematical Model. A computer simulation program was created using Python programming to solve the governing equations. The theoretical numerical simulation was tested in Excel to investigate the impact of operational parameters on performance and freshwater output. A thorough nonlinear differential equation model is used to explain the thermal transport and energy processes in the

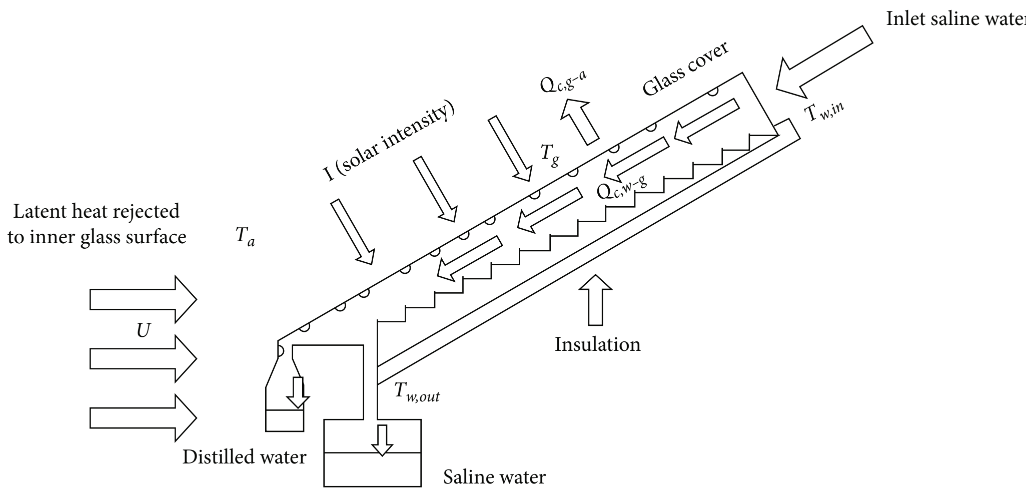

Figure 2: Energy distribution in stepping solar still.

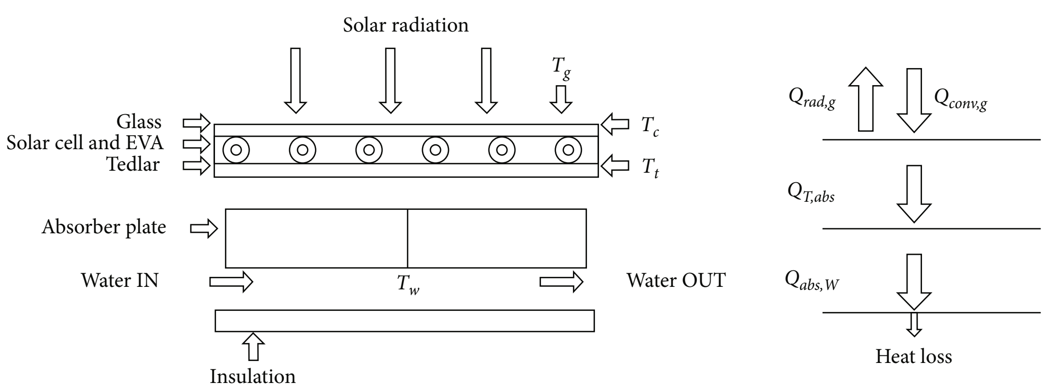

Figure 3: Schematic diagram of photovoltaic-thermal water collector with water and energy flow.

Table 1: Design parameters of a conventional solar stepped still [28, 29].

Design parameter	Value
ε_{eff}	0.85
Σ	0.0000000567 W/m^2.K^4
G	9.8 m/s
τ_g	0.95
A_w	1m^2
τ_w	0.95
ρ_w	997 kg/m^3
α_g	0.05
α_w	0.05
α_b	0.95
A_b	1m^2
$m_b c_{pb}$	12244.68
$m_w c_{pw}$	83760
$m_g c_{pg}$	6749.29416

active solar distillation system's main components. The volume of distilled water and the temperature of the condenser cover were calculated using these equations for various system configurations. By resolving the thermodynamic model by using energy balance equations for the system such as glass cover, salt water, and basin cover, the theoretical conclusions are reached.

The thermodynamic model is simplified by the following presumptions:

(1) The mass of the saline water, basin, and glass cover was constant

(2) Overall bottom heat transfer coefficient is kept constant

(3) The specific heat for all components is kept constant

(4) The glass cover temperature T_g was kept constant

The following are some significant still considerations utilized in the calculations: $F = 0.895$, $h_{p1} = 0.8772$, $h_{p2} = 0.9841$, $U_c = 8.6\,\text{W/m}^{2\circ}\text{C}$, $U_t = 9.24\,\text{W/m}^{2\circ}\text{C}$, $U_T = 66\,\text{W/m}^{2\circ}\text{C}$, $U_{tT} = 8.1028\,\text{W/m}^2\,{}^\circ\text{C}$, and $U_w = 500\,\text{W/m}^{2\circ}\text{C}$. The city of Vellore, Tamil Nadu, underwent a comparative examination in

Table 2: Assumed parameters for $I(t)$.

Assumed parameter	Value
γ_s (south)	0
β (tilt angle)	15°
n (22/06/21)	172
n (23/09/21)	265
n (20/12/21)	354
I_{sc} (maximum solar radiation outside atmosphere)	1367 W/m^2
ρ_r	0.2

Table 3: Design parameters of a PVT attached collector stepped still.

Design parameter	Value
$A_{c(\text{theoretical})}$	1.33 m^2
$A_{c(\text{exp})}$	0.77m^2
A_p	0.63 m^2
A_w	0.6 m^2
A_g	0.78 m^2
C_g	800 J/kg.°C
C_w	4200 J/kg.°C
C_p	450 J/kg.°C
C_f	0.38
D	0.05 m
h_{p-a}	5 W/m^2.°C
α_g	0.05
α_w	0.05
α_p	0.09
α_c	0.7
$(\alpha\tau)_{\text{eff}}$	0.66
ε_g	0.88
ε_w	0.95
η_{pump}	0.8
$\eta_{\text{el,ref}}$	0.1
τ_g	0.95
τ_w	0.95
h_{p1}	0.8872
$(\alpha\tau)_{\text{eff}}$	0.66
$\eta_{\text{el,ref}}$	0.1
U_T	66 W/m^2.°C
U_{tT}	8.1 W/m^2.°C
U_t	9.24 W/m^2.°C
U_w	500 W/m^2.°C

summer, winter, and rainy climatic conditions. Using data from the literature, the impact of operating factors on efficiency, productivity, and output power is evaluated.

4.3. Evaluation of Theoretical Observations. The theoretical calculations were done using existing temperature data and global solar radiations of the days 22/06/21 (for summer season), 20/12/21 (for winter season), and 23/09/21 (for rainy season) for the city of Vellore, Tamil Nadu.

Figure 7 illustrates the readings of solar radiation intensity for different climatic conditions. It has been found that the maximum solar radiation is around the noon hours (11 : 30 AM-1 : 30 PM). The recorded global solar radiation ranges for summer, winter, and rainy climatic conditions are 135.877 W/m^2–777.185 W/m^2, 59.392 W/m^2–527.52 W/m^2, and 107.069 W/m^2–547.862 W/m^2, respectively.

The variation of different components of the PVT-SSS is illustrated in Figure 8. During a sunny day, the ambient temperature increases post noon time (3 : 30 PM) and reaches around 35.64°C as shown in Figure 8. The variation of the glass cover temperature was from 28.06°C to 55.92°C throughout a summer day. In contrast on a cold day, the glass temperature ranged from 19.80°C to 44.92°C (Figure 9), and on a rainy day, the recorded minimum and maximum glass temperatures were found as 26.23°C and 39.25°C, respectively (Figure 10).

Similarly, Figure 9 depicts the winter, as the ambient temperature reaches a low of 19.81°C at 8 : 00 AM and subsequently drops to 27.64°C by 3 : 00 PM. On winter days, the basin plate temperature at midday reached 56°C (noon); on summer days, it reached 67°C (noon); and on wet days, it reached 47°C (1 o'clock).

During a rainy day, the ambient temperature attains a maximum of 31.75°C, and the minimum ambient temperature recorded was 26.23°C. Water temperature changes are also observed in all three different climatic conditions. The water temperature varied from 28.07°C to 64.58°C, 19.80°C to 54.11°C, and 26.23°C to 46.28°C in summer, winter, and rainy climatic conditions, respectively (Figures 8–10).

Figure 11 shows the comparison of the freshwater productivity by the PVT-SSS system throughout the day. For summer, winter, and rainy climatic circumstances, the freshwater productivity of PVT-SSS was determined to be 12.18 kg/m^{2}day, 6.67 kg/m^{2}day, and 2.770 kg/m^2 day, respectively. Freshwater production is shown to be substantially more on summer days than on winter and rainy days combined as the summer season receives the maximum solar radiation compared to other seasons.

Figure 12 illustrates the change in output electrical power over time. Throughout the experiment, the intensity of solar radiation varies. There is no uncertainty that when solar radiation rises, so does the output of electrical power. Also, in the three different climatic circumstances, the evaporation process was at its peak at midday, when the sun was shining the brightest. Hence, this leads to the generation of a maximum amount of electrical power. The energy generated on a summer day was found to be 9.91 kW/day. Similarly, on a winter day, it was around 6.52 kW/day, and on a rainy day, the energy generated was around 6.72 kW/day.

Table 4: For modeling validation: comparison of the experimental and analytical results in reference [5, 22].

Time	I	V_{wind}	t_a	$T_{c,\text{exp}}$ [25]	$T_{c,\text{cal}}$	$T_{w,\text{exp}}$ [28]	$T_{w,\text{cal}}$	$m_{\text{ev,exp}}$ [28]	$m_{\text{ev,cal}}$
8	272.83	0.58	21.42	21.12	23.72	21.12	21	0	0
08 : 30	350.78	1.23	23.7	32.42	39.57	37.34	38.28675	0.15	0.2
9	436.57	2.36	25.64	43.18	47.8	43.91	46.41324	0.35	0.42
09 : 30	525.92	3.42	27.18	49.19	52.86	47.92	50.99174	0.6	0.62
10	613.28	3.85	28.33	56.48	56.8	52.29	54.37292	0.75	0.784
10 : 30	692.23	3.77	29.15	60.13	60.17	57.21	57.25095	0.85	0.92
11	756.33	3.51	29.72	63.78	62.94	61.95	59.64435	0.96	1
11 : 30	799.88	3.14	30.16	68.15	65.11	65.05	61.60148	1.03	1.1
12	818.85	2.76	30.56	69.61	66.634	66.69	63.08162	1.06	1.147
12 : 30	811.42	2.5	30.96	71.25	67.31	68.58	63.89121	1.1	1.15
1	778.31	2.4	31.39	71.43	67.06	67.79	63.90457	1.07	1.129
01 : 30	772.63	2.38	31.8	69.79	66.44	66.88	63.18553	0.99	1.07
2	649.44	2.36	32.1	68.33	64.12	64.14	61.84511	0.9	0.983
02 : 30	564.97	2.3	32.16	65.23	61.64	61.95	59.91788	0.81	0.86
3	475.75	2.18	31.87	59.58	58.55	59.58	57.39984	0.68	0.738
03 : 30	387.78	2.02	31.13	54.66	54.86	55.39	54.23501	0.6	0.59
4	305.96	1.81	29.87	49.89	50.58	51.56	50.40746	0.47	0.46
04 : 30	233.66	1.59	28.1	44.87	45.75	45.55	45.91281	0.29	0.33
5	172.74	1.35	25.86	39.82	40.45	39.9	40.81258	0.19	0.22
Er (%)	—	—	—	0.62%		1.99%		6.77%	

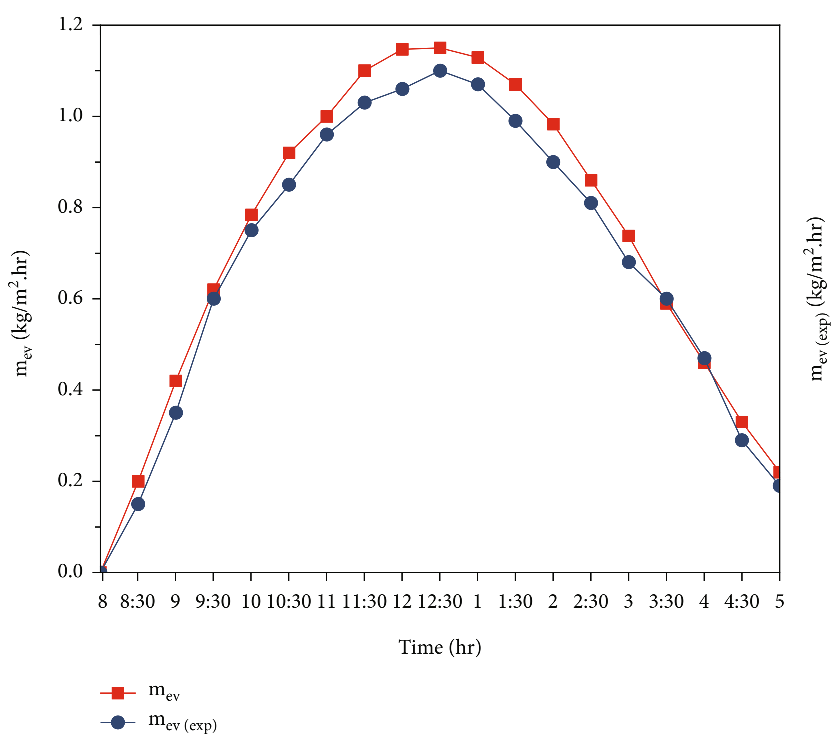

Figure 4: Freshwater productivity levels across time, as measured by simulations and experiments.

The noted electrical efficiency for summer, winter, and rainy climatic conditions are 8.91%, 9.53%, and 9.14% as shown in Figure 13. Because the PV cells are cooled by the salty water flow, their electrical efficiency does not agonize a considerable reduction. The summer season receives the most solar radiation; therefore, this season has the lowest electrical efficiency. This is due to the excessive increase of PV cells during this season.

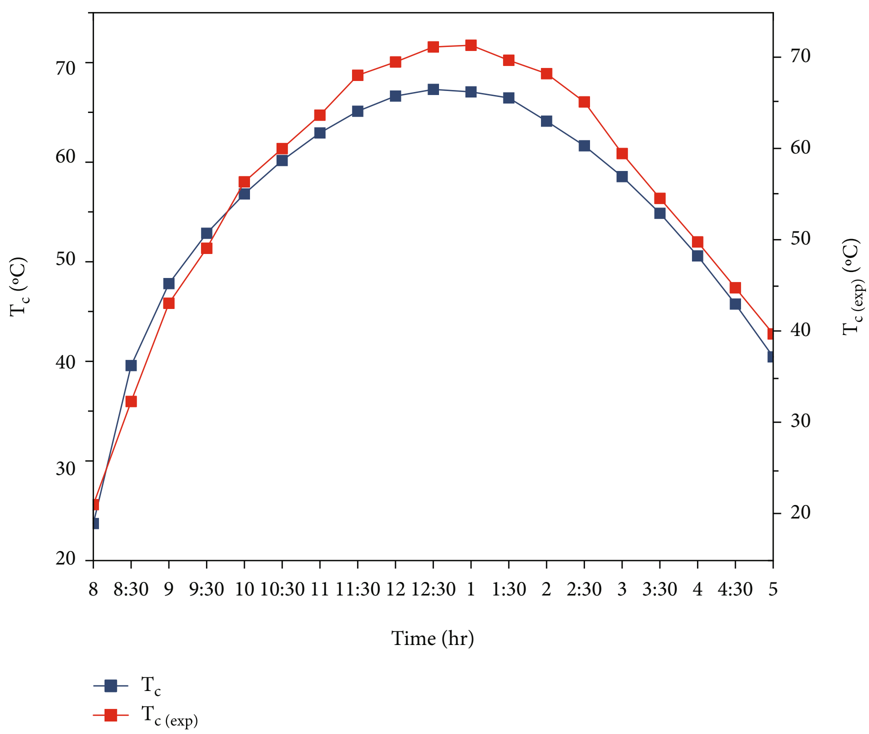

Figure 5: Temperature data of the PVT water collector shown against time using simulation and experiment.

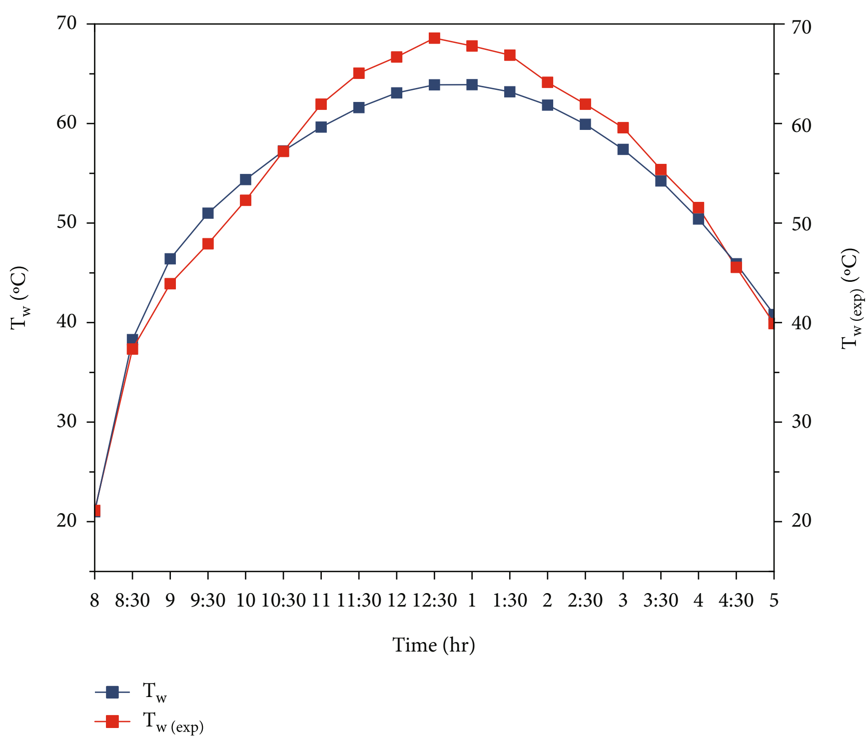

Figure 6: Experimental and simulated values of saline water temperature versus time.

The impact of depth of water production throughout the rainy season is seen in Figure 14. In 2 cm of water, the greatest rate of evaporation was seen. In 3 cm and 4 cm of water, the maximum rate of evaporation was observed at 331 kg/m^2 and 277 kg/m^2, respectively. Low volumetric heat capacity (C_p) is ensured by low water depth, which increases heat

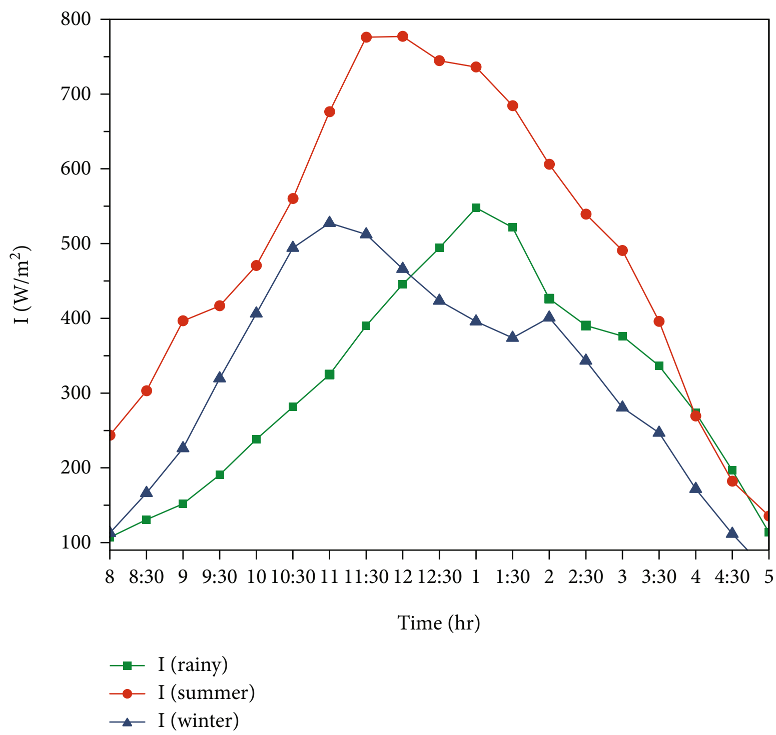

Figure 7: Hourly change of solar radiation intensity in summer, winter, and rainy climatic day conditions.

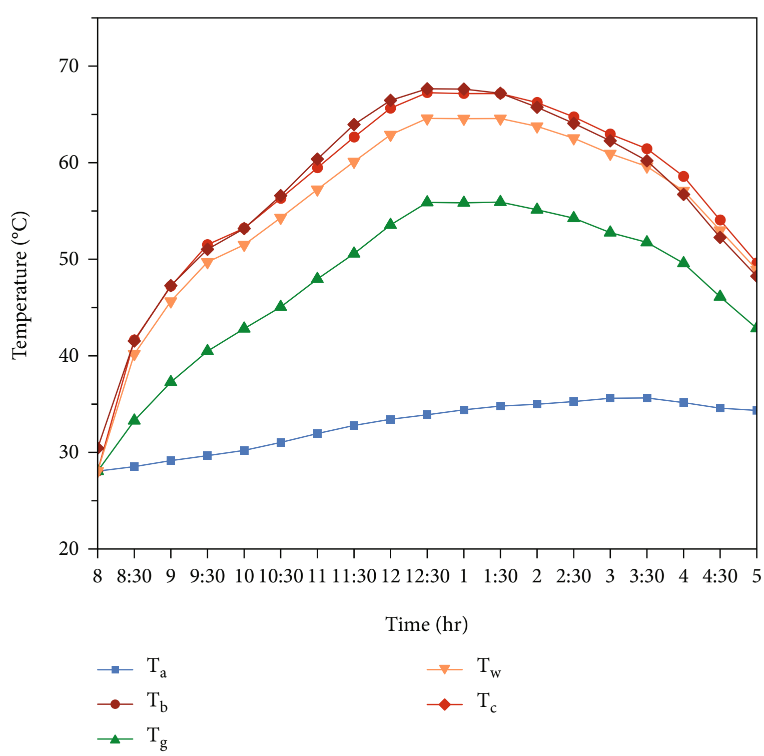

Figure 8: Temperature variations of PVT-SSS over time (summer climate).

transfer rather than heat storage. As a consequence, the salty water's temperature increases.

Figure 15 illustrates the effect of water depth productivity in the summer season. The highest evaporation rate was around 1668 kg/m^2 in 2 cm water depth, 1453 kg/m^2 in 3 cm water depth, and 1218 kg/m^2 in 5 cm water depth.

The impact of water depth production throughout the rainy season is seen in Figure 16. In 2 cm of water, 795 kg/

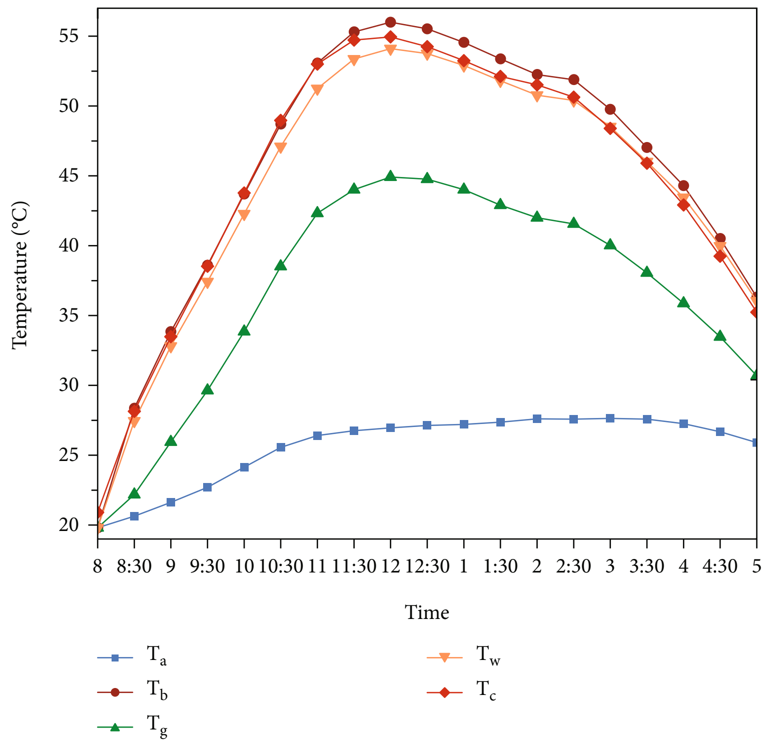

Figure 9: Temperature variations of PVT-SSS over time (winter climate).

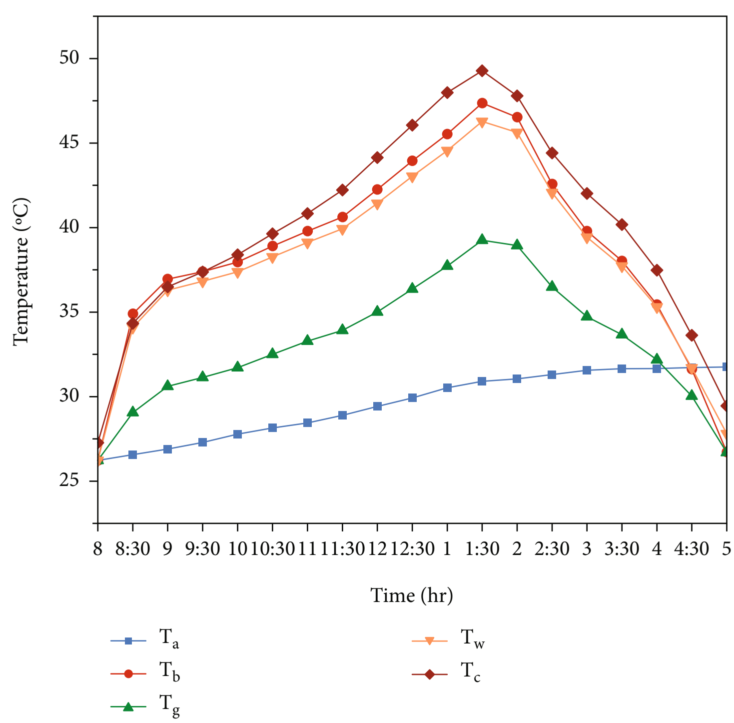

Figure 10: Temperature variations of PVT-SSS over time (rainy climate).

m^2 in 3 cm, and 667 kg/m^2 in 5 cm of water, the greatest evaporation rate of around 912 kg/m2 was observed.

Chiranjeevi and Srinivas [33] simulated a humidification dehumidification integrated into with vapor absorption refrigeration system. The simulation resulted in 25 LPH freshwater and 1 TR cooling at 250 m^3/h of airflow in the plant. The freshwater yielded from the experiments was tested for various parameters, and the results are as follows: from 1317 mg/L to 223.8 mg/L, the total dissolved solids (TDS) have reduced. The achieved pH for desalinated water is 7.2-7.5, which is in

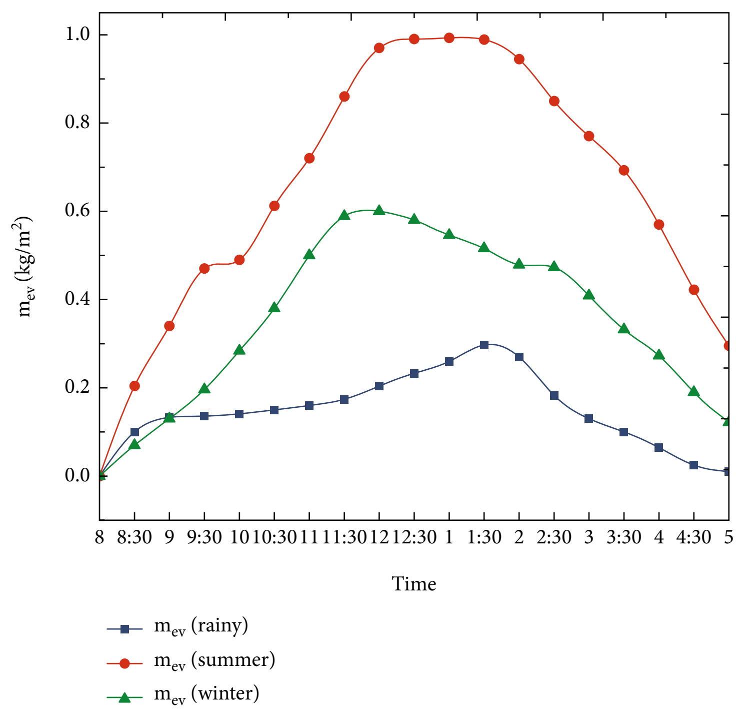

FIGURE 11: Freshwater productivity of PVT-SSS in winter, summer, and rainy climatic day conditions.

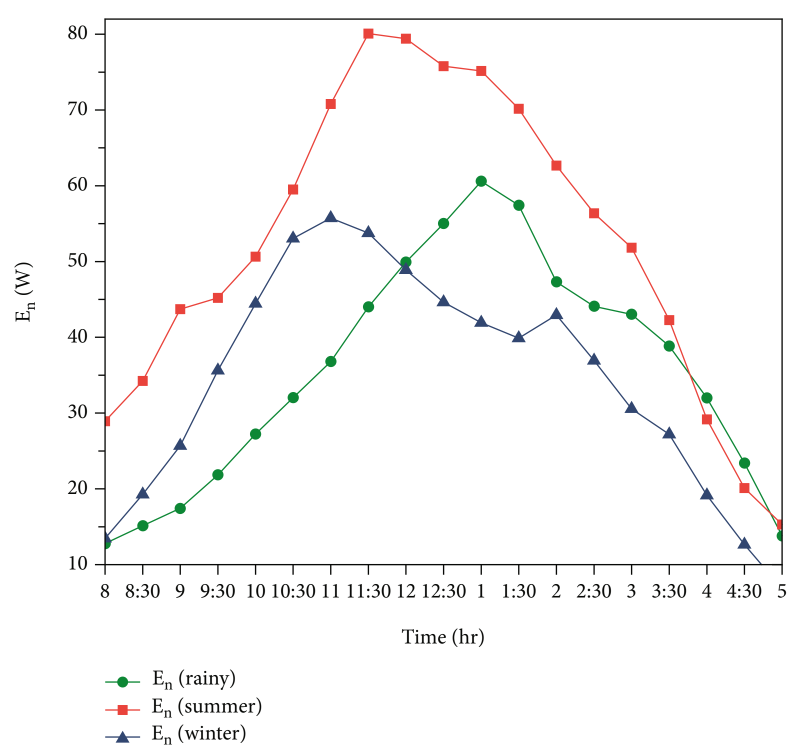

FIGURE 12: PVT-SSS output electrical power vs. test time in various climatic day situations.

a reasonable range. The desired pH is neutral, or 7, and the resulted pH is 7. Desalinated water's total hardness is reduced from 120 mg/L to 32 mg/L, and the produced turbidity ranges from 2.4 to 2.8 NTU. Additionally, the chlorides are reduced from 772.49 mg/L to 50 mg/L. There is a drop in sodium chloride from 3104 mg/L to 482.4 mg/L. Chemical oxygen demand (COD) analysis shows that the entire amount of compounds in the water can be oxidised. Water's COD is reduced from 80 mg/L to 60 mg/L, and its $CaCO_3$ hardness is reduced from 84 mg/L to 28 mg/L.

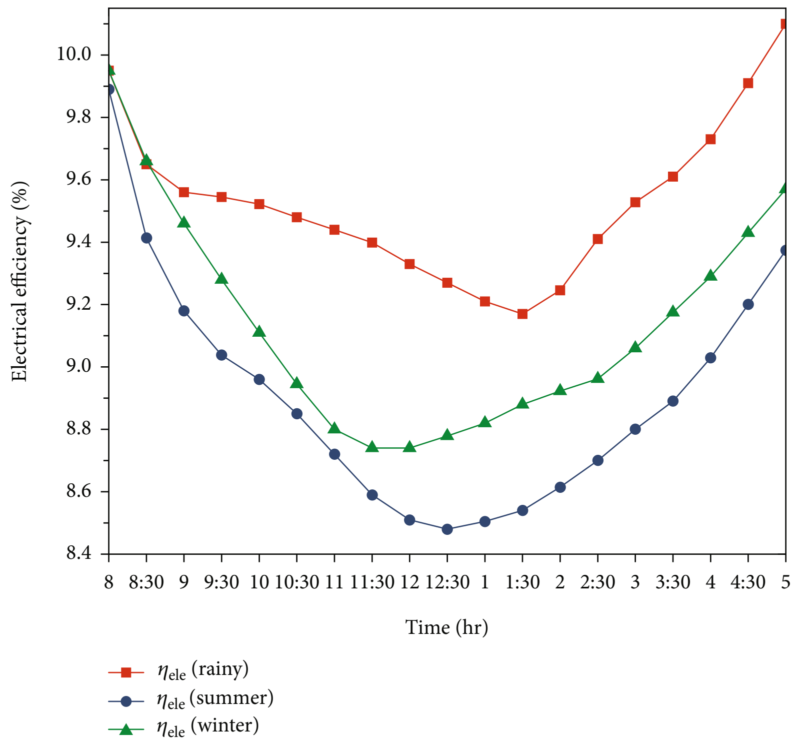

Figure 13: PVT-SSS electrical efficiency vs. time in various climatic day situations.

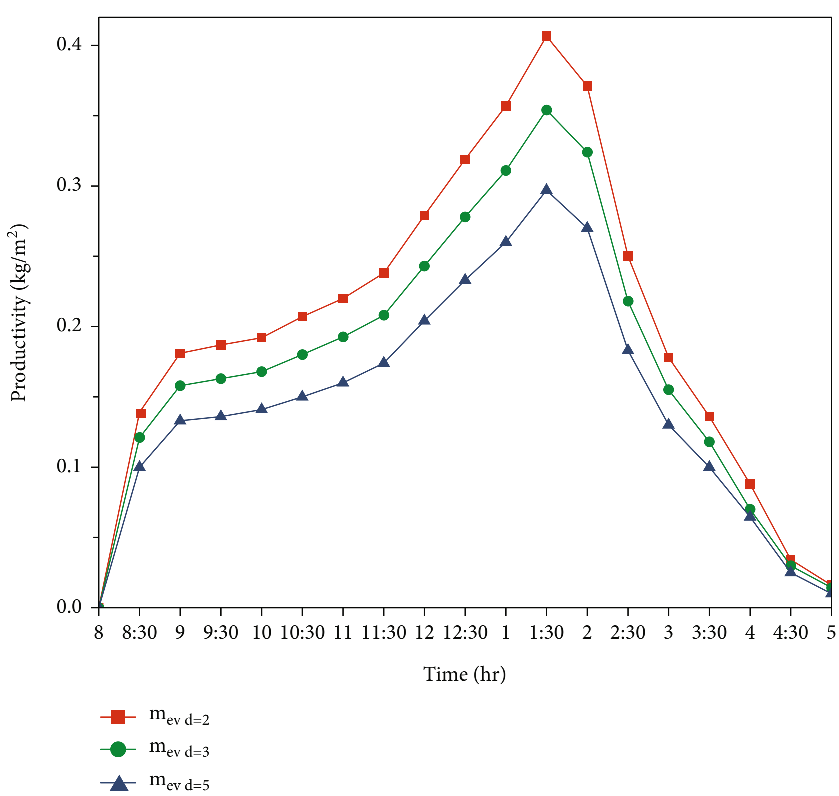

Figure 14: Effect of water depth productivity (rainy season).

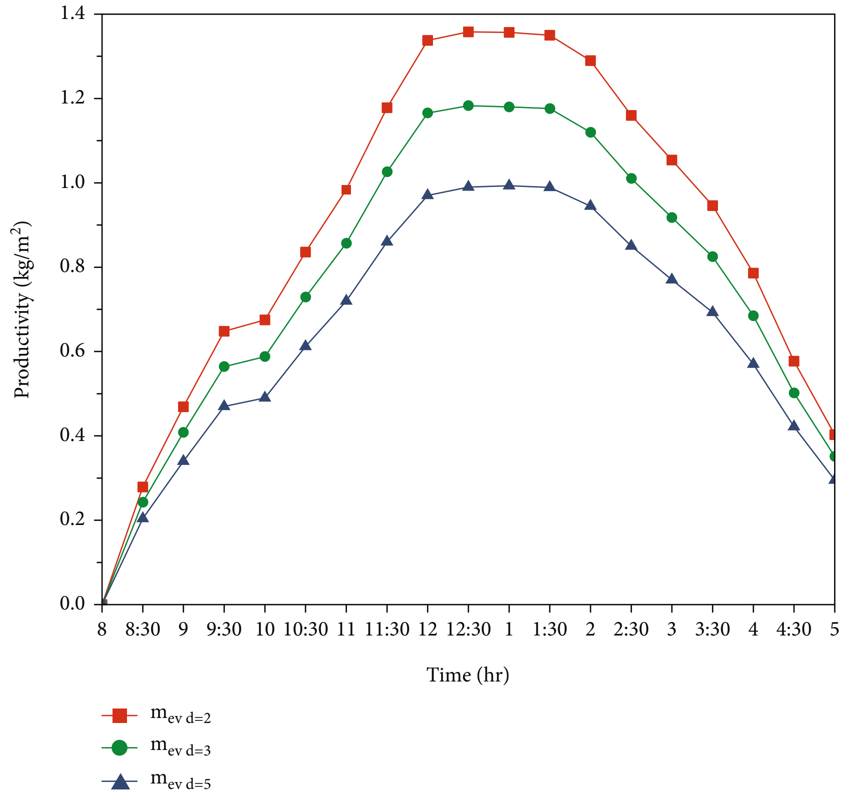

Figure 15: Effect of water depth productivity (summer season).

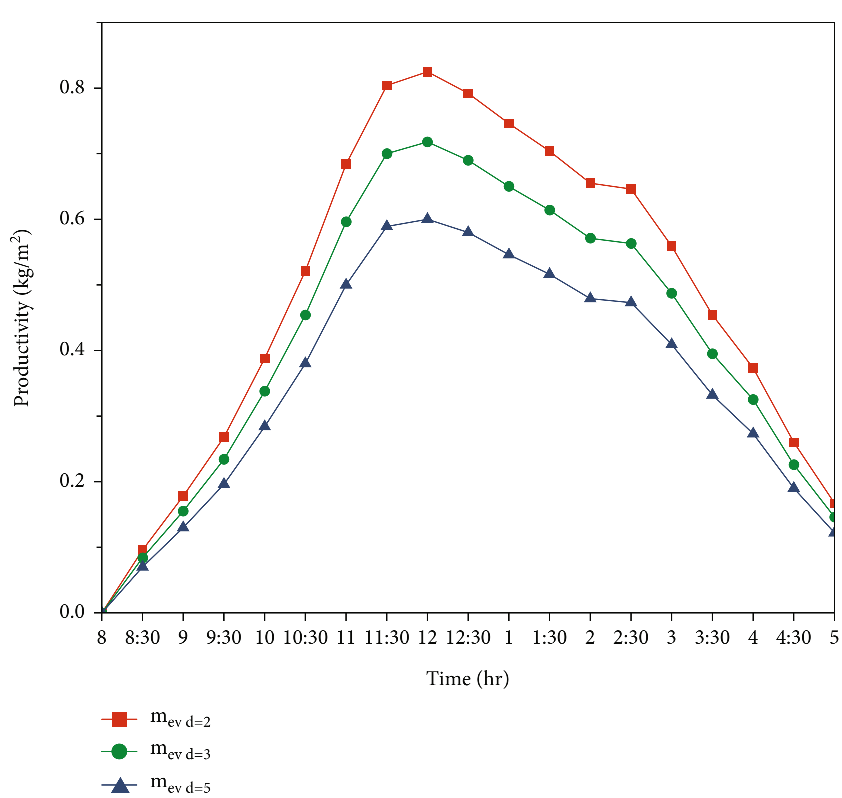

Figure 16: Effect of water depth productivity (winter season).

5. Conclusions

The following are the main conclusions of this study: using experimental data from the literature, the thermal model for PV/T coupled with stepped solar is verified, and the following are the key findings:

(i) In the summer season, the average electrical efficiency is 8.91% generating 9.91 kW/day (approx.) along with freshwater productivity of 12.18 kg/m^2 day

(ii) In the rainy season, the average electrical efficiency is 9.53% generating 6.72 kW/day (approx.) along with freshwater productivity of 2.77 kg/m^2 day

(iii) In the winter season, the average electrical efficiency is 9.135% generating 6.52 kW/day (approx.) along with freshwater productivity of 6.67 kg/m^2 day

(iv) The PVT-SSS system employed different water levels of 2 cm, 3 cm, and 5 cm, and the summer months had the highest yield. The lowest output 1218 kg/m^2 is produced at a water depth of 5 cm, while the maximum production of 1668 kg/m^2 is produced at a 2 cm depth of water

(v) A theoretical model of PVT stepped solar and empirical observations continue to agree well. When the PVT water collection is coupled to the stepped solar still, both energy efficiency and freshwater output are boosted by two times

(vi) The PVT collector in the hybrid active solar still also supplies power for pumps for other uses throughout the day's sunlight

Nomenclature

α: Absorptivity
β: Tilt angle
$\varepsilon_{\mathrm{eff}}$: Effective remittances
E: Emissivity
μ: Viscosity (N·s/m^2)
η: Efficiency (%)
σ: Stefan Boltzmann constant (W/m^2K^4)
τ: Transmissivity
D: Water depth
t: Time
I: Global solar radiation (W/m^2)
$Q_{c,w-g}$: Energy going in the glass includes the reflected energy from the basin water through convection
$Q_{e,w-g}$: Energy going in the glass includes the reflected energy from the basin water through evaporation
$Q_{r,w-g}$: Energy going in the glass includes the reflected energy from the basin water through radiation
h: Latent heat of vaporization
A: Area (m^2)
C: Heat capacity of water in the basin (J/K)
h_c: Convective heat transfer coefficient (W/m^2K)
h_{fg}: Latent heat of evaporation (W/m^2K)
h_w: Wind heat-transfer coefficient (W/m^2K)
d: Water depth (m)
$h_{c,g-\mathrm{sky}}$: Convective heat transfer coefficient between glass and atmosphere (W/m^2K)
$h_{c,w-g}$: Conductive heat transfer coefficient from glass inner surface to glass outer surface (W/m^2K)
$h_{e,w-g}$: Evaporative heat transfer coefficient from water and an inner surface of the glass cover (W/m^2K)
$h_{r,g-\mathrm{sky}}$: Radiation heat transfer coefficient between glass and atmosphere (W/m^2K)
$h_{r,w-g}$: Radiation heat transfer coefficient from water to glass cover inner surface (W/m^2K)
$h_{t,w-g}$: Total heat transfer coefficient from water to glass cover inner surface (W/m^2K)
h_w: Convective heat transfer coefficient between basin liner and water mass (W/m^2K)
k: Thermal conductivity (W/m K)
m_{ev}: Hourly productivity of distilled water from SS (kg/m^2h)
P: Pressure (Pa)
Q: Heat gain (W/m^2)
T: Temperature (°C)
U: Overall heat loss coefficient (W/m^2K).

Subscripts

a: Ambient
c: Collector
eff: Effective
el: Electrical
en: Energy
ev: Evaporative
exp: Experimental
g: Glass cover
i: i-th parameter
loss: Loss
r: Radiative
t: Top
T: Tedlar
tT: Tedlar or top
th: Thermal
sky: Sky
w: Water, wind
in: Input
out: Output
cv: Volume control.

Acronyms and abbreviations

PVT: Hybrid photo voltaic thermal
SS: Solar still
SSS: Stepped solar still
PCM: Phase change materials
PV/T: Photovoltaic/thermal
STEPS: State political scenario.

Data Availability

All the data has been included within the manuscript.

Conflicts of Interest

The authors declare that they have no conflicts of interest.

Acknowledgments

The authors thank the financial support provided by the VIT, Vellore, India, through the SEED grant SG20210279 to Dr. C. Chiranjeevi, Associate Professor, School of Mechanical Engineering.

References

[1] R. Hofste, P. Reig, and L. Schleifer, *17 Countries*, Home to One-Quarter of the World's Population, Face Extremely High Water Stress, 2019.

[2] C. Chiranjeevi and T. Srinivas, "Experimental and simulation studies on two stage humidification- dehumidification desalination and cooling plant," *Desalination*, vol. 376, pp. 9–16, 2015.

[3] WHO/UNICEF Joint Water Supply and Sanitation Monitoring Programme, *Progress on drinking water and sanitation: 2014 update*, World Health Organization., 2014.

[4] G. Hulton and World Health Organization, *Global Costs and Benefits of Drinking-Water Supply and Sanitation Interventions to Reach the MDG Target and Universal Coverage (No. WHO/HSE/WSH/12.01)*, World Health Organization, 2012.

[5] C. Chiranjeevi and T. Srinivas, "Combined two stage desalination and cooling plant," *Desalination*, vol. 345, pp. 56–63, 2014.

[6] L. Cozzi and T. Gould, "World Energy Outlook," vol. 2021, pp. 1–383, 2021, https://iea.blob.core.windows.net/assets/4ed140c1-c3f3-4fd9-acae-789a4e14a23c/WorldEnergyOutlook2021.pdf.

[7] S. Malavika, C. Chiranjeevi, Y. R. Sekhar et al., "Performance optimization of a heat pump for high temperature application," *Materials Today: Proceedings*, vol. 46, pp. 5278–5285, 2021.

[8] Z. Fan, J. Ren, H. Bai et al., "Shape-controlled fabrication of MnO/C hybrid nanoparticle from waste polyester for solar evaporation and thermoelectricity generation," *Chemical Engineering Journal*, vol. 451, article 138534, 2023.

[9] J. Ren, Y. Ding, J. Gong, J. Qu, and R. Niu, "Simultaneous solar-driven steam and electricity generation by cost-effective, easy-scale up MnO_2-based flexible membranes," *Energy & Environmental Materials.*, 2022.

[10] C. Chiranjeevi, T. Srinivas, and R. Shankar, "Experimental investigation on a hybrid desalination and cooling unit using humidification-dehumidification technique," *Desalin Water Treatment*, vol. 156, pp. 148–160, 2019.

[11] M. Naroei, F. Sarhaddi, and F. Sobhnamayan, "Efficiency of a photovoltaic thermal stepped solar still: experimental and numerical analysis," *Desalination*, vol. 441, pp. 87–95, 2018.

[12] A. Riahi, K. W. Yusof, B. S. M. Singh, E. Olisa, N. Sapari, and M. H. Isa, "The performance investigation of triangular solar stills having different heat storage materials," *International Journal of Energy and Environmental Engineering*, vol. 6, no. 4, pp. 385–391, 2015.

[13] A. Riahi, Y. K. Wan, B. S. Mahinder Singh, M. H. Isa, E. Olisa, and N. A. Zahari, "Sustainable potable water production using a solar still with photovoltaic modules-AC heater," *Desalination Water Treat*, vol. 57, no. 32, pp. 14929–14944, 2016.

[14] S. Jasrotia, A. Kansal, and V. V. N. Kishore, "Application of solar energy for water supply and sanitation in arsenic affected rural areas: a study for Kaudikasa village, India," *Journal of Cleaner Production*, vol. 60, pp. 102–106, 2013.

[15] A. Ahsan, M. Imteaz, U. A. Thomas, M. Azmi, A. Rahman, and N. N. Nik Daud, "Parameters affecting the performance of a low cost solar still," *Applied Energy*, vol. 114, pp. 924–930, 2014.

[16] S. B. Sadineni, R. Hurt, C. K. Halford, and R. F. Boehm, "Theory and experimental investigation of a weir-type inclined solar still," *Energy*, vol. 33, no. 1, pp. 71–80, 2008.

[17] R. U. Khan, B. Bhattacharyya, and G. Singh, "Experimental study of modified dual slope hybrid photovoltaic (PV/T) solar thermal still," *Desalination and Water Treatment*, vol. 156, pp. 168–176, 2019.

[18] P. K. Ng and N. Mithraratne, "Lifetime performance of semi-transparent building-integrated photovoltaic (BIPV) glazing systems in the tropics," *Renewable and Sustainable Energy Reviews*, vol. 31, pp. 736–745, 2014.

[19] N. Kahoul, M. Houabes, and M. Sadok, "Assessing the early degradation of photovoltaic modules performance in the Saharan region," *Energy Conversion and Management*, vol. 82, pp. 320–326, 2014.

[20] M. Abdolzadeh and M. Ameri, "Improving the effectiveness of a photovoltaic water pumping system by spraying water over the front of photovoltaic cells," *Renewable Energy*, vol. 34, no. 1, pp. 91–96, 2009.

[21] S. Jamali, M. Yari, and S. M. S. Mahmoudi, "Enhanced power generation through cooling a semi-transparent PV power plant with a solar chimney," *Energy Conversion and Management*, vol. 175, pp. 227–235, 2018.

[22] B. M. Zilli, A. M. Lenz, S. N. M. de Souza et al., "Performance and effect of water-cooling on a microgeneration system of photovoltaic solar energy in Parana, Brazil," *Journal of Cleaner Production*, vol. 192, pp. 477–485, 2018.

[23] P. Iodice, G. Langella, and A. Amoresano, "Energy performance and numerical optimization of a screw expander–based solar thermal electricity system in a wide range of fluctuating operating conditions," *International Journal of Energy Research*, vol. 44, no. 3, pp. 1858–1874, 2020.

[24] P. Iodice, A. Amoresano, G. Langella, and F. S. Marra, "Combined use of volumetric expanders and Scheffler receivers to improve the efficiency of a novel direct steam solar power plant," *International Journal of Energy Research*, vol. 45, no. 15, pp. 21058–21081, 2021.

[25] D. P. Winston, P. Pounraj, A. M. Manokar, R. Sathyamurthy, and A. E. Kabeel, "Experimental investigation on hybrid PV/T active solar still with effective heating and cover cooling method," *Desalination*, vol. 435, pp. 140–151, 2018.

[26] J. Ji, J. P. Lu, T. T. Chow, W. He, and G. Pei, "A sensitivity study of a hybrid photovoltaic/thermal water-heating system with natural circulation," *Applied Energy*, vol. 84, no. 2, pp. 222–237, 2007.

[27] S. Kumar and G. N. Tiwari, "Life cycle cost analysis of single slope hybrid (PV/T) active solar still," *Applied Energy*, vol. 86, no. 10, pp. 1995–2004, 2009.

[28] M. S. S. Abujazar, S. Fatihah, E. R. Lotfy, A. E. Kabeel, and S. Sharil, "Performance evaluation of inclined copper-stepped solar still in a wet tropical climate," *Desalination*, vol. 425, pp. 94–103, 2018.

[29] E. Hedayati-Mehdiabadi, F. Sarhaddi, and F. Sobhnamayan, "Energy analysis of a stepped cascade solar still connected to photovoltaic thermal collector," *International Journal of Automotive & Mechanical Engineering*, vol. 14, no. 4, pp. 4805–4825, 2017.

[30] R. Sathyamurthy, D. G. Harris Samuel, and P. K. Nagarajan, "Theoretical analysis of inclined solar still with baffle plates for improving the fresh water yield," *Process Safety and Environmental Protection*, vol. 101, pp. 93–107, 2016.

[31] A. Tiwari and M. S. Sodha, "Performance evaluation of solar PV/T system: an experimental validation," *Solar Energy*, vol. 80, no. 7, pp. 751–759, 2006.

[32] A. Alaudeen, K. Johnson, P. Ganasundar, A. Syed Abuthahir, and K. Srithar, "Study on stepped type basin in a solar still," *Journal of King Saud University - Engineering Sciences*, vol. 26, no. 2, pp. 176–183, 2014.

[33] C. Chiranjeevi and T. Srinivas, "Dessalement augmente avec refroidissement," *International Journal of Refrigeration*, vol. 80, pp. 106–119, 2017.